



Altered Functional Brain Networks in Patients with Traumatic Anosmia: Resting-State Functional MRI Based on Graph Theoretical Analysis

Mina Park, MD, PhD^{1, 2*}, Jinyong Chung, PhD^{3*}, Jin Kook Kim, MD, PhD⁴, Yong Jeong, MD, PhD³, Won-Jin Moon, MD, PhD¹

Departments of ¹Radiology and ⁴Otorhinolaryngology-Head and Neck Surgery, Konkuk University Medical Center, Konkuk University School of Medicine, Seoul, Korea; ²Department of Radiology, Gangnam Severance Hospital, Yonsei University College of Medicine, Seoul, Korea; ³Laboratory for Cognitive Neuroscience and NeuroImaging, Department of Bio and Brain Engineering, and KI for Health Science and Technology, Korea Advanced Institute of Science and Technology (KAIST), Daejeon, Korea

Objective: Traumatic anosmia is a common disorder following head injury; however, little is known regarding its neural basis and influence on the functional networks. Therefore, we aimed to investigate the functional connectivity changes in patients with traumatic anosmia compared to healthy controls using resting-state functional magnetic resonance imaging (rs-fMRI).

Materials and Methods: Sixteen patients with traumatic anosmia and 12 healthy controls underwent rs-fMRI. Differences in the connectivity of the olfactory and whole brain networks were compared between the two groups. Graph theoretical parameters, such as modularity and global efficiency of the whole brain or olfactory networks, were calculated and compared. Correlation analyses were performed between the parameters and disease severity.

Results: Patients with traumatic anosmia showed decreased intra-network connectivity in the olfactory network (false discovery rate [FDR]-corrected $p < 0.05$) compared with that in healthy controls. Furthermore, the inter-network connectivity was increased in both the olfactory (FDR-corrected $p < 0.05$) and whole brain networks (degree-based statistic-corrected $p < 0.05$) in the anosmia group. The whole brain networks showed decreased modularity ($p < 0.001$) and increased global efficiency ($p = 0.019$) in patients with traumatic anosmia. The modularity and global efficiency were correlated with disease severity in patients with anosmia ($p < 0.001$ and $p = 0.002$, respectively).

Conclusion: Traumatic anosmia increased the inter-network connectivity observed with rs-fMRI in the olfactory and global brain functional networks. rs-fMRI parameters may serve as potential biomarkers for traumatic anosmia by revealing a more widespread functional damage than previously expected.

Keywords: Traumatic anosmia; Functional magnetic resonance imaging; Resting state; Brain networks; Functional connectivity; Graph theory

Received February 6, 2019; accepted after revision July 16, 2019.

This study was supported by the Basic Science Research Program through the National Research Foundation of Korea funded by the Korean Government (NRF-2016R1D1A1B01012705), and a grant of the Korea Health Technology R&D Project through the Korea Health Industry Development Institute (KHIDI), funded by the Ministry of Health & Welfare, Republic of Korea (grant number HI18C1038).

*These authors contributed equally to this work.

Corresponding author: Won-Jin Moon, MD, PhD, Department of Radiology, Konkuk University Medical Center, Konkuk University School of Medicine, 120-1 Neungdong-ro, Gwangjin-gu, Seoul 05030, Korea.

• Tel: (822) 2030-7619 • Fax: (822) 2030-7469 • E-mail: mdmoonwj@naver.com; and

Yong Jeong, MD, PhD, Laboratory for Cognitive Neuroscience and NeuroImaging, Department of Bio and Brain Engineering, and KI for Health Science and Technology, Korea Advanced Institute of Science and Technology, 291 Daehak-ro, Yuseong-gu, Daejeon 34141, Korea.

• Tel: (8242) 350-4324 • Fax: (8242) 350-4310 • E-mail: yong@kaist.ac.kr

This is an Open Access article distributed under the terms of the Creative Commons Attribution Non-Commercial License (<https://creativecommons.org/licenses/by-nc/4.0>) which permits unrestricted non-commercial use, distribution, and reproduction in any medium, provided the original work is properly cited.

INTRODUCTION

Traumatic anosmia is a common disorder following head injury and is known to affect approximately 5–14.5% of patients with head trauma (1, 2). Traumatic anosmia has been shown to affect the patients' quality of life (3). Although olfactory dysfunction after trauma is thought to be mostly caused by a direct damage to the olfactory nerve and the associated nerve center (4), a traumatic incident without any structural abnormality can also lead to clinically overt olfactory dysfunction (5).

Functional magnetic resonance imaging (fMRI) can be used to measure the functional activity or functional connectivity in patients with smell disorders and can enhance our fundamental understanding of how the olfactory system works (6-9). Therefore, findings from fMRI studies may lead to better prognostication and improved treatment strategies (6-9). Previous fMRI studies have demonstrated that the administration of odors results in decreased activation of the olfactory brain regions in patients with smell disorders and olfactory dysfunction (6, 10-12). While task-based fMRI can provide additional information regarding brain function, task instructions can be difficult for patients with olfactory dysfunction due to accompanying cognitive problems. Furthermore, odor-stimulated task-based fMRI studies have provided various results due to the heterogeneity of olfactory tasks, overlapping functional areas responsible for sniffing and olfaction, and habituation of the olfactory systems (13).

Unlike task-based fMRI, resting-state fMRI (rs-fMRI) appears to be a promising evaluation tool for understanding the functional activity and connectivity without specific stimuli or tasks (14). In this respect, rs-fMRI may have additional benefits compared to odor-stimulated task-based fMRI for the evaluation of olfactory dysfunction in patients with smell disorder. rs-fMRI studies on olfactory dysfunction have been rarely reported to date, specifically in those with post-traumatic anosmia (7, 15). Therefore, the objective of this study was to investigate the differences in the functional connectivity between patients with traumatic anosmia and healthy controls using rs-fMRI. We hypothesized that patients with traumatic anosmia would have specific disruptions in the network connectivity within the whole brain as well as in the olfactory networks when compared to healthy controls and that these alteration patterns would be related to the symptom severity.

MATERIALS AND METHODS

Study Population

This prospective study was approved by the ethics committee of Konkuk University Medical Center. Sixteen patients (mean age, 43.2 ± 10.2 years; 11 males) with traumatic anosmia were included in the study between November 2012 and May 2014. The inclusion criteria were as follows: 1) presentation within 2 years of head injury; 2) fulfilment of criteria for anosmia based on the Korean Version of the Sniffin' stick (KVSS) II test; and 3) age between 18 and 65 years. The exclusion criteria were as follows: 1) history of olfactory impairment; 2) history of sinonasal disease; or 3) current nasal symptoms. All patients completed psychophysical olfactory testing, including the KVSS I and II, and underwent nasal endoscopy to exclude the possibility of obstructive olfactory loss.

Twelve healthy controls (mean age, 26.8 ± 8.4 years; 8 males) were also recruited from the local community. The inclusion criteria for healthy controls were as follows: 1) normal olfactory function; 2) no brain lesions or prior head trauma; and 3) no history of psychiatric or neurologic diseases. All study participants were right-handed. All participants provided written informed consent prior to study participation.

Clinical Olfactory Assessment

An otorhinolaryngologist with 17 years of clinical experience performed the endoscopic examination of the nasal cavity and the clinical olfactory performance testing in all patients to ensure that patients met the criteria for anosmia. Clinical olfactory performance measures included the KVSS I and II. The KVSS I test is a modified Sniffin' stick test optimized for Korean patients, which includes odors familiar to Korean individuals, and the KVSS II is the Korean equivalent of the Sniffin' stick test (16, 17). Clinical diagnosis of anosmia was based on the KVSS II scores; total scores between 0–20 were classified as anosmia, scores of 20.25–27 were classified as hyposmia, and scores of 27.25–48 were classified as normosmia (16, 17).

MRI Acquisition

All participants underwent MRI using a 3T MR scanner (Signa HDxT; GE Healthcare, Milwaukee, WI, USA) with an 8-channel head coil. High spatial resolution T1-weighted three-dimensional (3D) anatomic images were obtained in the axial plane using a fast-spoiled gradient echo sequence

(repetition time [TR]: 7.8 ms; echo time [TE]: 3.0 ms; matrix: 256 x 256; flip angle: 13°; number of sections: 134; field of view: 240 x 240 mm²; section thickness: 1.3 mm).

rs-fMRI was performed in the axial plane using a gradient-echo echo-planar imaging (EPI) sequence (TR: 2000 ms; TE: 30 ms; matrix: 64 x 64; flip angle: 90; number of sections: 40; field of view: 240 x 240 mm; section thickness: 3.5 mm; scan of volume: 800) with a voxel size of 3.75 x 3.75 x 3.5 mm.

fMRI Data Pre-Processing

fMRI data pre-processing was performed using SPM12 (Wellcome Trust Centre for Neuroimaging, London, UK) and in-house codes of MATLAB R2016b (MathWorks, Natick, MA, USA). The first three volumes of each dataset were discarded to allow for equilibration effects. We performed slice timing correction to realign fMRI slices of each scan to the first slice that was the reference slice based on its relative timing within the entire scan. Then, spatial realignment was performed to remove movement artifacts from the fMRI data. Scans were spatially realigned to a reference scan in order to revise any spatial mismatches caused by movement (18). We chose the first scan as the reference scan and used the default option of SPM12 (quality: 0.9; separation: 4; smoothing: 5; interpolation: 2nd degree). fMRI scans from each subject were then co-registered to their T1-weighted 3D anatomic images (19). The default option of SPM12 (objective function: normalized mutual information; histogram smoothing: 7) was used here as well. Next, steps were taken to reduce the noise signals. All scans were temporally band-pass filtered (0.01–0.08 Hz) to remove slow signal drifts (20, 21). Brain tissues were segmented using the co-registered T1-weighted MRI scans, and white matter and cerebrospinal fluid signals were extracted. We linearly regressed out the white matter and cerebrospinal fluid signals, while the linear temporal trends and motion parameters acquired from the realignment step (six parameters) were also considered as nuisance parameters. Finally, we performed spatial normalization to the EPI template with a 2-mm slice thickness of the MNI space (Montreal Neurological Institute: International Consortium for Brain Mapping) and spatial smoothing with the 4-mm full-width at half-maximum Gaussian kernel.

Brain Networks

In this study, we used a total of 279 functional areas for brain network analysis. We further added the olfactory

network to the pre-defined whole brain network.

First, the pre-defined whole brain network suggested by Jonathan Power and colleagues was constructed with 264 functional areas (22). Those areas were then divided into 12 predefined well-known networks, involved in different cognitive processes. Among the 264 functional areas, 33 areas with uncertain network classifications were also included (22). Next, the olfactory network was defined by statistical localization (23). The olfactory network was comprised of 21 functional areas including the piriform cortex, insular cortex, prefrontal cortex, and anterior cingulate/frontal cortex (Supplementary Table 1). All regions-of-interest (ROIs) were near-sphere in shape (3 x 3 x 3 cube with an additional voxel on the center of each face, total 33 voxels) and located at their center. Six ROIs from the pre-defined whole brain network were discarded as they overlapped with the ROIs from the olfactory network. A final check was performed to ensure there were no overlapping voxels between the ROIs.

Functional Connectivity and Whole Brain Network Analysis

Functional connectivity was measured as the Pearson correlation coefficient between the ROI time-series. The whole brain network with 279 x 279 connectivity was constructed. We used binary network type for calculating the network properties, where the connectivity of p value < 0.05 (positive and significant correlation) takes the value of 1, otherwise the connectivity takes the value of 0 (24).

Two network properties were measured to explore functional integration and segregation (25, 26). Global efficiency is a measure of how efficiently a network exchanges information. Global efficiency has been suggested as a measure of functional integration and is calculated as the inverse of the harmonic mean of the shortest path length in the network:

$$\text{Global efficiency} = \frac{1}{n(n-1)} \sum_{\substack{i,j \in G \\ i \neq j}} \frac{1}{d_{ij}}$$

Where d_{ij} is the shortest path length connecting nodes i and j , and G represents the graph.

Modularity is a statistical unit that quantifies the degree of network subdivision into clearly delineated modules. The Louvain community detection algorithm was applied to construct modules in the network (27). The Louvain algorithm optimizes and constructs the modules to

maximize the modularity of the network.

$$\text{Modularity} = \frac{1}{2n} \sum_{ij} [K_{ij} - \frac{k_i k_j}{2n}] \delta(c_j, c_i)$$

Where n is the number of all edges in the graph, K_{ij} is the binary value of the edge between nodes i , and j . k_i and k_j are the number of the edges attached to nodes i and j . c_i and c_j represent the modules of the nodes and δ is a simple delta function.

Structural MRI Analysis

A neuroradiologist with 20 years of experience who was blinded to the clinical data assessed the images from the T1-weighted fast-spoiled gradient echo sequence for structural brain abnormalities. For assessment, multi-planar reformatted images as well as original axial images were used. When tissue loss was present, the maximal dimension of the tissue loss was measured on a picture archiving and communication system (Centricity Enterprise Imaging, GE Healthcare, Barrington, IL, USA).

Statistical Analyses

To compare the demographic variables between patients with anosmia and healthy controls, the nonparametric Mann-Whitney test and Fisher's exact test were used due to our small sample size using the Statistical Package for the Social Sciences (SPSS, version 23.0, IBM Corp., Armonk, NY, USA). P values less than 0.05 were considered to be statistically significant.

Statistical analysis for the rs-fMRI data was performed in MATLAB using in-house codes. All group comparisons were tested using a two sample t test after controlling for age difference between the groups. The age effect unaffected by the disease was estimated by linear regression for the healthy controls and was controlled for both groups (28). Individual functional connectivity was tested using Student's t distribution and was transformed into p values to determine whether the functional connectivity was significant in the brain networks. Functional connectivity comparison within networks was further tested in consideration for multiple comparisons. False discovery rate (FDR) was controlled in the olfactory network comparison (29, 30). For the other comparisons, we adopted a cluster-wise inference method, a degree-based statistic to find clusters significantly influenced by the disease (31). Finally, multiple linear regression was used to evaluate the

explanatory power of the network properties in predicting the behavioral scores of patients.

RESULTS

Demographics and Clinical and Imaging Features

The mean age of the patients with traumatic anosmia was significantly greater than that of healthy controls ($p < 0.001$), with no significant difference in the sex ratio ($p = 1.000$). The mean time between head injury and clinical consultation was 9.6 months (range, 3–24 months) in the anosmia group. Four of the 16 patients exhibited focal encephalomalacia on the structural MRI, with the maximum dimension ranging from < 1.0 cm in 3 patients to approximately 3.0 cm in one patient; the lesions were located at both gyri recti ($n = 1$), the left gyrus rectus ($n = 2$), or the right gyrus rectus ($n = 1$). The patient with the largest lesion showed involvement of the left medial orbital gyrus as well. There were no additional structural abnormalities in the brains of all subjects. In patients with anosmia, the mean KVSS II score was 9.44 ± 3.7 (range, 3–15), indicating that all patients met the diagnostic criteria for anosmia.

Changes in Olfactory Network in Patients with Traumatic Anosmia

Compared with healthy controls, patients with anosmia exhibited different patterns of connectivity in the olfactory network (Fig. 1). Intra-cluster connectivity was decreased in patients, specifically in the insular cortex and anterior cingulate/frontal cortex (FDR-corrected $p < 0.05$). Inter-anatomical-cluster connectivity (across piriform cortex, insular cortex, prefrontal cortex, anterior cingulate/frontal cortex) was increased in the patients compared with that in the healthy controls (FDR-corrected $p < 0.05$).

Comparison of Whole Brain Functional Connectivity

Patients with traumatic anosmia showed increased connectivity in most brain regions (Figs. 2, 3) compared with that in healthy controls. Furthermore, the functional connectivity in the patients was primarily increased among the thalamic and sensory networks (visual and somatomotor hand) compared with the healthy controls (Table 1).

Comparison of Functional Network Organization

Compared with healthy controls, patients with traumatic anosmia showed significantly increased global efficiency

(0.753 ± 0.056 vs. 0.704 ± 0.042) ($p = 0.019$) and decreased modularity (0.165 ± 0.044 vs. 0.245 ± 0.054) ($p < 0.001$) in the whole brain network.

Correlation between Network Parameters and KVSS II Score

In patients with traumatic anosmia, the global efficiency

of the whole brain network was significantly correlated with the KVSS II score ($r^2 = 0.71$, $p = 0.002$) and remained significant after controlling for disease duration ($r^2 = 0.75$, $p < 0.001$) (Fig. 4). Modularity of the whole brain network was also significantly associated with the KVSS II score ($r^2 = 0.79$, $p < 0.001$) and remained significant after controlling for disease duration ($r^2 = 0.82$, $p < 0.001$).

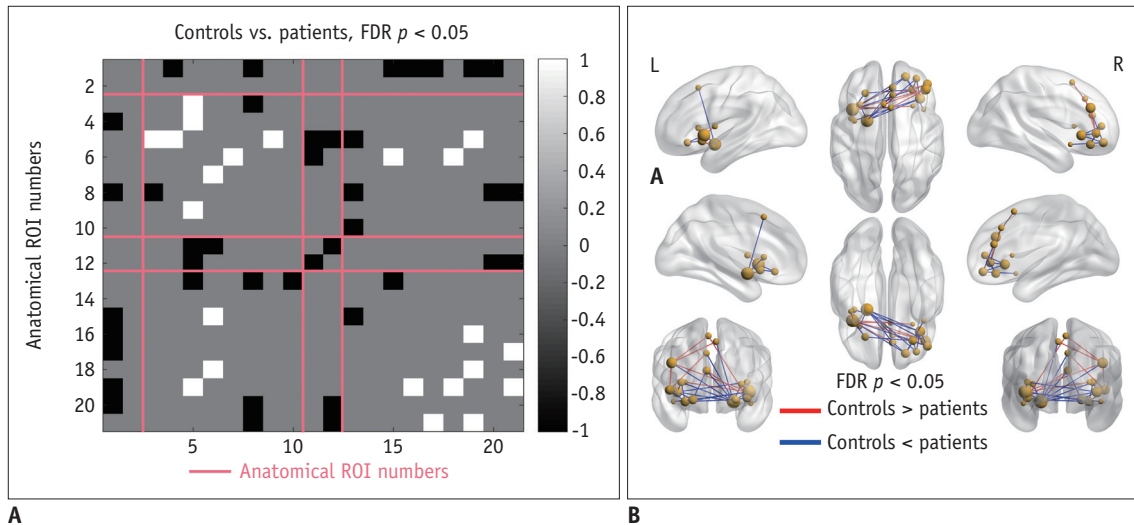


Fig. 1. Functional connectivity of olfactory network and functional connectivity differences between healthy controls and patients with traumatic anosmia. Numbers in left column and bottom row indicate anatomical ROI numbers, and information about each ROI number is provided in Supplementary Table 1.

A. Significant difference in functional connectivity between groups. White color indicates significantly lower functional connectivity and black color indicates significantly higher functional connectivity in patients. Intra-cluster connectivity was decreased in patients, specifically in insular cortex (ROI numbers 4, 5, 8, and 10) and anterior cingulate/frontal cortex (ROI numbers 13, 15, 16, 17, 19, 20, and 21). Inter-anatomical-cluster connectivity was increased in patients (ROI numbers 3, 4, 5, 6, 7, 9, 15, 18, and 19). **B.** Glass-brain representation of functional connectivity differences. Both higher and lower functional connectivity were observed in patients with anosmia compared to that in healthy controls. FDR = false discovery rate, ROI = region-of-interest

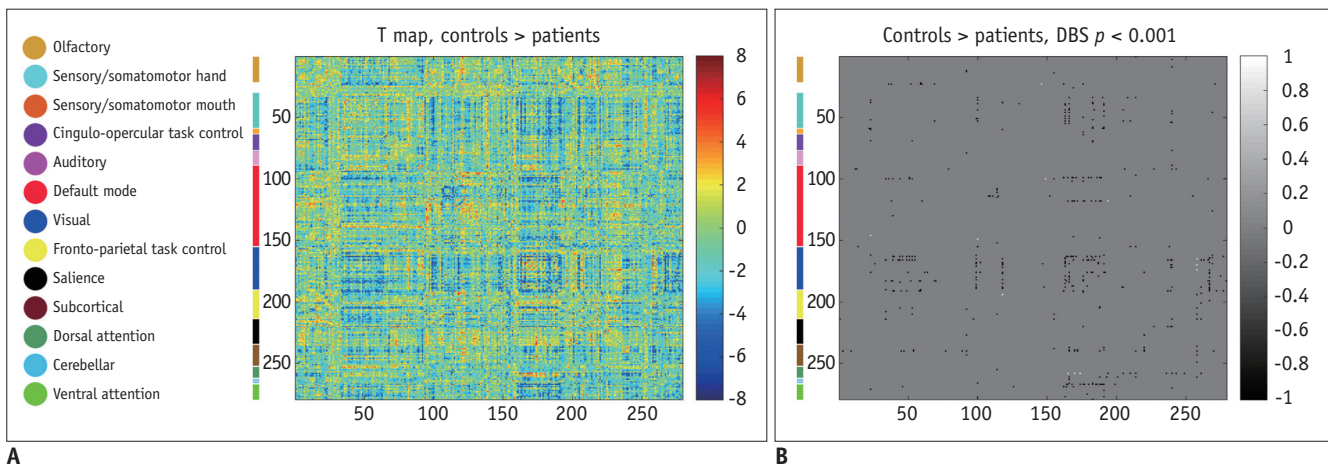


Fig. 2. Whole brain functional connectivity and differences between healthy controls and patients with traumatic anosmia. **A.** Functional connectivity differences are shown as t-statistic matrix, where positive values indicate lower connectivity in patients and vice versa. **B.** Functional connectivity with significant difference between groups through cluster-wise inference methods. White color indicates significantly lower functional connectivity and black color indicates significantly higher functional connectivity in patients with anosmia with corresponding anatomic locations appearing on color blocks and each color indicating different anatomic functional location from one shown in left column. Functional connectivity was generally higher in significant clusters for patients. DBS = degree-based-statistic

DISCUSSION

In this study, we demonstrated that the intra-network connectivity of the olfactory network was decreased in patients with anosmia compared with that in healthy controls, whereas the inter-network connectivity of both olfactory and whole-brain networks was increased. These findings may suggest that the compensatory mechanism, which is based on the recruitment of other brain areas, partly plays a role in the evolution of traumatic olfactory dysfunction as previously suggested in many

neurodegenerative and psychiatric diseases (32-34).

Indeed, there is strong evidence supporting brain plasticity in response to pathological damage induced by various insults (34), as well as in the case of olfactory dysfunction (32, 35). The results of a previous study on anosmia revealed diverse network changes, involving mostly non-olfactory regions, the prefrontal areas, the left inferior frontal gyrus, and the left premotor cortex (35). In addition to plasticity as it relates to functional loss, the reorganization and establishment of new connections have been demonstrated at the cognitive level of the

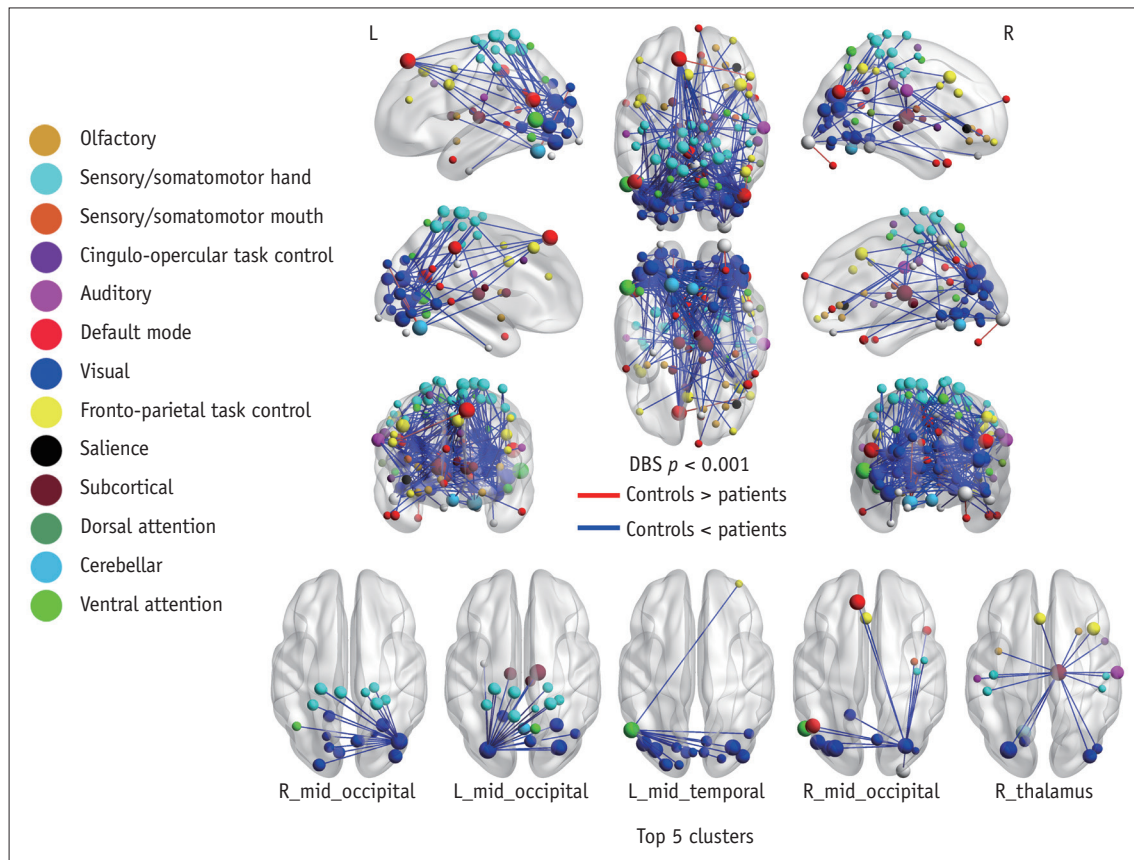


Fig. 3. Glass brain representations of functional connectivity differences. Nodes are highlighted with various colors according to their assigned networks. Edges in blue indicate lower connectivity, while red indicates higher connectivity in patients. Top 5 clusters are presented separately in bottom figure. Cluster presented on left was more significant. Additional information on clusters is provided in Table 1. Major clusters had significant functional connectivity differences between visual, sensory/somatomotor hand, and subcortical networks.

Table 1. Information of Top Clusters with Increased Functional Connectivity in Whole-Brain Analysis

Top 5 Clusters	ROI Number	Network Classification	Anatomical Label	x	y	z	Weighted Degree
1	163	Visual	Right middle occipital	40	-72	14	19
2	166	Visual	Left middle occipital	-28	-79	19	16
3	267	Ventral attention	Left middle occipital	-52	-63	5	14
4	176	Visual	Right middle occipital	29	-77	25	12
5	240	Subcortical	Right thalamus	12	-17	8	10

ROI = region-of-interest

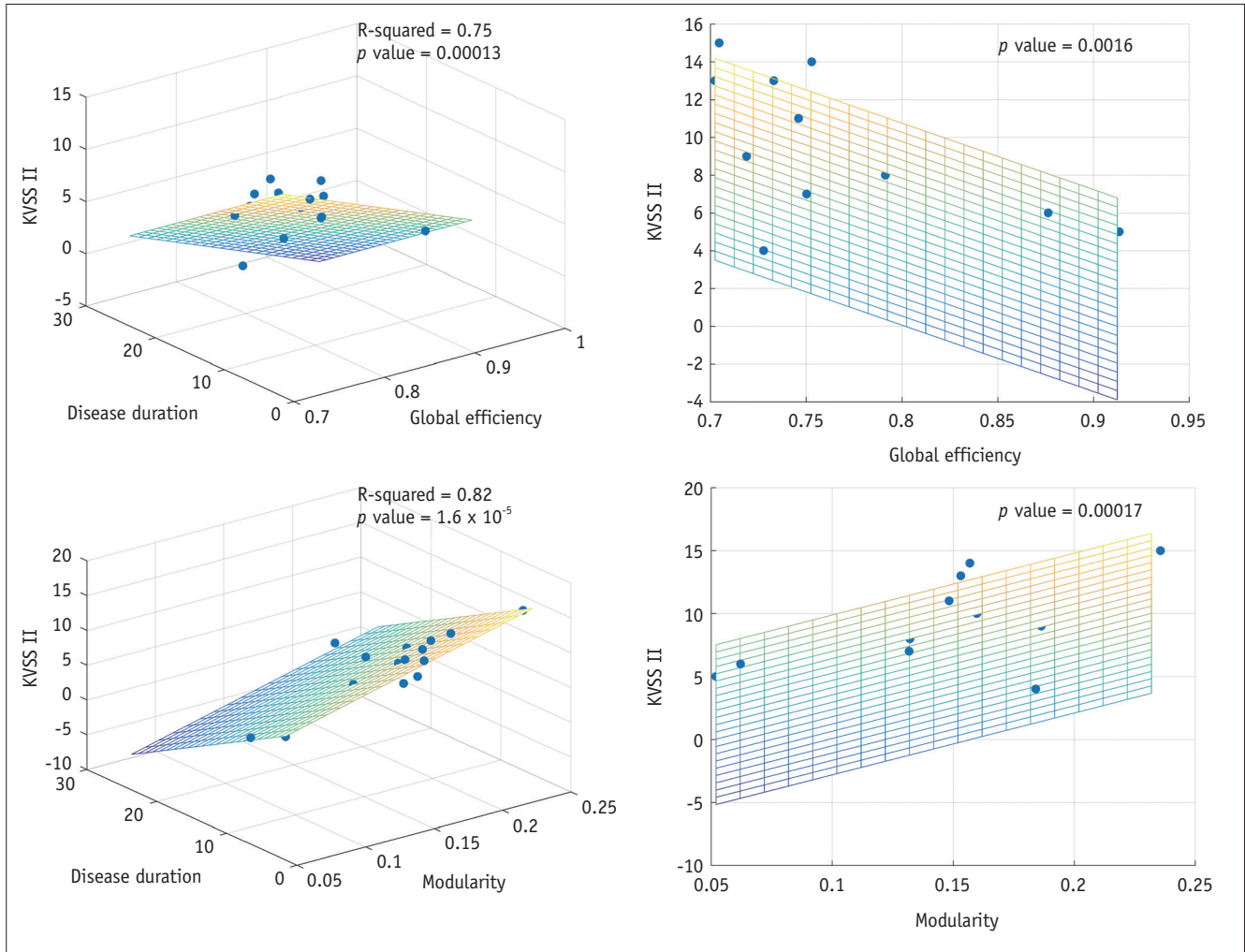


Fig. 4. Predicting KVSS II score using network parameters for patients with traumatic anosmia. Three-dimensional scatter plots show linear relationships between KVSS II score, network parameters, and disease duration. Network parameters predicted KVSS II scores when controlling for disease duration. R-squared and *p* values of whole regression model, and *p* value for each parameter are presented. Global efficiency and modularity showed significant and opposite linear relationships with KVSS II score. KVSS = Korean Version of Sniffin stick

olfactory system, although the underlying mechanisms behind the plasticity of the olfactory system are still under investigation (35, 36). Furthermore, a structural analysis in patients with traumatic anosmia has also revealed paradoxical increases in gray matter volume according to disease duration (32), giving another line of evidence for the compensatory mechanism after olfactory dysfunction. Therefore, we believe that an impaired activation of the olfactory network, manifesting as a decreased intra-network connectivity of the olfactory network, may induce a compensatory activation of other networks as observed in our study.

However, our finding is not entirely consistent with the observations of previous studies that investigated the

effects of olfactory disorders or neurodegenerative disorders presenting as olfactory dysfunction at the early stage. They reported a decreased activation in the olfactory areas of the brain, using odor-stimulated task-based fMRI (6, 12). Yet, the functional connectivity and network properties beyond the olfactory areas have not been studied until recently. Kollndorfer et al. (7) first reported task-based fMRI connectivity analysis, which revealed decreased functional connectivity in the somatosensory and integrative networks as well as the olfactory network. In contrast to the previous report, we observed that functional connectivity was prominently increased in the motor and visual cortex in addition to the inter-network connectivity of the olfactory network and that in the somatosensory networks.

This discrepancy may be due to differences in the study methodology, as the previous study used task-related fMRI for the olfactory, integrative, and somatosensory networks, whereas we analyzed the whole brain connectivity with 279 different functional networks while using rs-fMRI for the first time.

To clearly understand the dynamic interaction among different brain regions, we performed a graph theory-based network analysis, which can offer a better understanding of the local and global organization of resting-state networks (37). Specifically, we used two of the most popular measures: global efficiency and modularity. Global efficiency indicates how effectively information is integrated across the entirety of the networks. Conversely, modularity indicates how effectively information is integrated between immediate neighboring brain regions of a given network node (38).

We found that global efficiency was increased while modularity (modular organization) was decreased in patients with traumatic anosmia compared with those in healthy controls. With respect to modularity, our finding is consistent with previous observations showing that modularity decreases with normal aging (39, 40), neuropsychiatric disorders, such as schizophrenia (41), and preclinical Alzheimer's disease (42). Modularity can be large when nodes are maximally connected within a module, but minimally connected between modules (42). Accordingly, the decreased modularity in the patients with traumatic anosmia indicates a less distinctive functional modular structure than that in the normal group, and this alteration of network could be a manifestation of a compensatory mechanism either from an increase in intermodular connections, a decrease in intramodular connections, or a combination of both (40).

The increased global efficiency of the resting-state connectivity in patients can be explained by the increased functional connectivity of the whole brain networks for adapting to the local damage responsible for olfactory core dysfunction. In many networks, modularity and global efficiency are inversely related and this is consistent with what we observed in our study (43). As the brain is a complex network, an increased global efficiency with decreased modularity reflects a less organized connectivity and a more random network (44). We speculated that although the brain of patients with traumatic anosmia attempts to overcome impairment derived from olfactory dysfunction by increasing the functional connectivity both

within and outside the olfactory network, disorganized and increased randomization within the networks may hinder the perfect compensation to these damages.

When interpreting our findings, however, we should not ignore the potential effect of concomitant brain pathology from non-olfactory traumatic brain injury. It has been reported that diffuse microstructural and functional changes can be present even without overt structural abnormality in patients with mild traumatic brain injury (45, 46). The reported results of these invisible changes, however, are inconsistent in terms of functional connectivity. Some studies reported decreased global efficiency and increased modularity in patients with mild traumatic brain injury and posttraumatic stress disorder (47, 48). Conversely, several recent studies reported an increase in the resting functional connectivity after traumatic concussion relative to the controls (49, 50), which is in line with our findings. Thus, our findings may represent a pattern of the dynamics behind functional connectivity changes following trauma as well as a representation of the olfactory dysfunction itself.

It is worth noting that global efficiency and modularity were found to have a significant correlation with the severity of olfactory dysfunction based on the KVSS II score in our study. This suggests that a lower degree of organization in the brain network, expressed as decreased modularity and increased global efficiency, is correlated with the clinical severity in traumatic anosmia. This may support the claim that olfactory dysfunction is the major contributor to the connectivity changes observed in our study. Furthermore, given the relationship between these two measures and the clinical severity, we believe that these two measures can be used as imaging biomarkers to objectively evaluate the clinical status of subjects with traumatic anosmia in the future.

There are several limitations in this study. Although this study recruited a relatively small study population, we found statistically significant differences in the rs-fMRI analysis, even after multiple comparison corrections. Second, the difference in the age between the groups might have contributed to the results, but we included the age as a covariate in the analyses to minimize the effect of age differences. Furthermore, there was a significant correlation between disease severity and rs-fMRI derived parameters, indicating that the changes in the anosmia group are likely induced by the disease itself rather than aging. Third, cerebromalacia in the orbitofrontal cortex was present, albeit in a small number from the whole population and this

might subsequently have affected the connectivity changes in the rs-fMRI.

In conclusion, we present rs-fMRI evidence of traumatic anosmia-induced connectivity changes in the global functional networks and olfactory functional networks. These findings suggest that rs-fMRI parameters, by revealing more widespread functional damage than previously expected, may serve as potential biomarkers for traumatic anosmia.

Supplementary Materials

The Data Supplement is available with this article at <https://doi.org/10.3348/kjr.2019.0104>.

Conflicts of Interest

The authors have no potential conflicts of interest to disclose.

ORCID iDs

Won-Jin Moon

<https://orcid.org/0000-0002-8925-7376>

Yong Jeong

<https://orcid.org/0000-0002-5907-3787>

Mina Park

<https://orcid.org/0000-0002-2005-7560>

Jinyong Chung

<https://orcid.org/0000-0001-9473-5152>

Jin Kook Kim

<https://orcid.org/0000-0003-4245-6252>

REFERENCES

- Costanzo RM, Miwa T. Posttraumatic olfactory loss. *Adv Otorhinolaryngol* 2006;63:99-107
- Mott AE, Leopold DA. Disorders in taste and smell. *Med Clin North Am* 1991;75:1321-1353
- Schofield PW, Moore TM, Gardner A. Traumatic brain injury and olfaction: a systematic review. *Front Neurol* 2014;5:5
- Miao X, Yang L, Gu H, Ren Y, Chen G, Liu J, et al. Evaluation of post-traumatic anosmia with MRI and chemosensory ERPs. *Eur Arch Otorhinolaryngol* 2015;272:1945-1953
- Yousem DM, Geckle RJ, Bilker WB, McKeown DA, Doty RL. Posttraumatic olfactory dysfunction: MR and clinical evaluation. *AJNR Am J Neuroradiol* 1996;17:1171-1179
- Henkin RI, Levy LM. Functional MRI of congenital hyposmia: brain activation to odors and imagination of odors and tastes. *J Comput Assist Tomogr* 2002;26:39-61
- Kollndorfer K, Fischmeister FP, Kowalczyk K, Hoche E, Mueller CA, Trattning S, et al. Olfactory training induces changes in regional functional connectivity in patients with long-term smell loss. *Neuroimage Clin* 2015;9:401-410
- Moon WJ, Park M, Hwang M, Kim JK. Functional MRI as an objective measure of olfaction deficit in patients with traumatic anosmia. *AJNR Am J Neuroradiol* 2018;39:2320-2325
- Reichert JL, Postma EM, Smeets PAM, Boek WM, de Graaf K, Schöpf V, et al. Severity of olfactory deficits is reflected in functional brain networks-An fMRI study. *Hum Brain Mapp* 2018;39:3166-3177
- Hummel T, Fliebsbach K, Abele M, Okulla T, Reden J, Reichmann H, et al. Olfactory FMRI in patients with Parkinson's disease. *Front Integr Neurosci* 2010;4:125
- Schneider F, Habel U, Reske M, Toni I, Falkai P, Shah NJ. Neural substrates of olfactory processing in schizophrenia patients and their healthy relatives. *Psychiatry Res* 2007;155:103-112
- Wang J, Eslinger PJ, Doty RL, Zimmerman EK, Grunfeld R, Sun X, et al. Olfactory deficit detected by fMRI in early Alzheimer's disease. *Brain Res* 2010;1357:184-194
- Vedaei F, Fakhri M, Harirchian MH, Firouznia K, Lotfi Y, Ali Oghabian M. Methodological considerations in conducting an olfactory fMRI study. *Behav Neurol* 2013;27:267-276
- Hohenfeld C, Werner CJ, Reetz K. Resting-state connectivity in neurodegenerative disorders: is there potential for an imaging biomarker? *Neuroimage Clin* 2018;18:849-870
- Kollndorfer K, Jakab A, Mueller CA, Trattning S, Schöpf V. Effects of chronic peripheral olfactory loss on functional brain networks. *Neuroscience* 2015;310:589-599
- Hong SC, Yoo YS, Kim ES, Kim SC, Park SH, Kim JK, et al. Development of KVSS test (Korean version of Sniffin' Sticks test). *Korean J Otorhinolaryngol-Head Neck Surg* 1999;42:855-860
- Cho JH, Jeong YS, Lee YJ, Hong SC, Yoon JH, Kim JK. The Korean version of the Sniffin' stick (KVSS) test and its validity in comparison with the cross-cultural smell identification test (CC-SIT). *Auris Nasus Larynx* 2009;36:280-286
- Friston K, Harrison L, Daunizeau J, Kiebel S, Phillips C, Trujillo-Barreto N, et al. Multiple sparse priors for the M/EEG inverse problem. *Neuroimage* 2008;39:1104-1120
- Collignon A, Maes F, Delaere D, Vandermeulen D, Suetens P, Marchal G. *Automated multi-modality image registration based on information theory*. In: Bizais Y, Barillot C, Di Paola R, eds. *Information processing in medical imaging*. Dordrecht: Kluwer Academic Publishers, 1995:263-274
- Rao H, Korkczykowski M, Pluta J, Hoang A, Detre JA. Neural correlates of voluntary and involuntary risk taking in the human brain: an fMRI study of the Balloon Analog Risk Task (BART). *Neuroimage* 2008;42:902-910
- Shah C, Erhard K, Ortheil HJ, Kaza E, Kessler C, Lotze M. Neural correlates of creative writing: an fMRI study. *Hum Brain Mapp* 2013;34:1088-1101
- Power JD, Cohen AL, Nelson SM, Wig GS, Barnes KA, Church

- JA, et al. Functional network organization of the human brain. *Neuron* 2011;72:665–678
23. Seubert J, Freiherr J, Djordjevic J, Lundström JN. Statistical localization of human olfactory cortex. *Neuroimage* 2013;66:333-342
 24. Pamplona GS, Santos Neto GS, Rosset SR, Rogers BP, Salmon CE. Analyzing the association between functional connectivity of the brain and intellectual performance. *Front Hum Neurosci* 2015;9:61
 25. Rubinov M, Sporns O. Complex network measures of brain connectivity: uses and interpretations. *Neuroimage* 2010;52:1059-1069
 26. Latora V, Marchiori M. Efficient behavior of small-world networks. *Phys Rev Lett* 2001;87:198701
 27. Blondel VD, Guillaume JL, Lambiotte R, Lefebvre E. Fast unfolding of communities in large networks. *J Stat Mech* 2008;2008:P10008
 28. Chung J, Yoo K, Lee P, Kim CM, Roh JH, Park JE, et al. Normalization of cortical thickness measurements across different T1 magnetic resonance imaging protocols by novel W-score standardization. *Neuroimage* 2017;159:224-235
 29. Groppe DM, Urbach TP, Kutas M. Mass univariate analysis of event-related brain potentials/fields I: a critical tutorial review. *Psychophysiology* 2011;48:1711-1725
 30. Benjamini Y, Hochberg Y. Controlling the false discovery rate: a practical and powerful approach to multiple testing. *J R Stat Soc B* 1995;57:289-300
 31. Yoo K, Lee P, Chung MK, Sohn WS, Chung SJ, Na DL, et al. Degree-based statistic and center persistency for brain connectivity analysis. *Hum Brain Mapp* 2017;38:165-181
 32. Han P, Winkler N, Hummel C, Hähner A, Gerber J, Hummel T. Alterations of brain gray matter density and olfactory bulb volume in patients with olfactory loss after traumatic brain injury. *J Neurotrauma* 2018;35:2632-2640
 33. Damoiseaux JS, Prater KE, Miller BL, Greicius MD. Functional connectivity tracks clinical deterioration in Alzheimer's disease. *Neurobiol Aging* 2012;33:828.e19-e30
 34. Bettus G, Guedj E, Joyeux F, Confort-Gouny S, Soulier E, Laguitton V, et al. Decreased basal fMRI functional connectivity in epileptogenic networks and contralateral compensatory mechanisms. *Hum Brain Mapp* 2009;30:1580-1591
 35. Kollndorfer K, Kowalczyk K, Hoche E, Mueller CA, Pollak M, Trattng S, et al. Recovery of olfactory function induces neuroplasticity effects in patients with smell loss. *Neural Plast* 2014;2014:140419
 36. Bende M, Nordin S. Perceptual learning in olfaction: professional wine tasters versus controls. *Physiol Behav* 1997;62:1065-1070
 37. van den Heuvel MP, Hulshoff Pol HE. Exploring the brain network: a review on resting-state fMRI functional connectivity. *Eur Neuropsychopharmacol* 2010;20:519-534
 38. Stanley ML, Simpson SL, Dagenbach D, Lyday RG, Burdette JH, Laurienti PJ. Changes in brain network efficiency and working memory performance in aging. *PLoS One* 2015;10:e0123950
 39. Meunier D, Achard S, Morcom A, Bullmore E. Age-related changes in modular organization of human brain functional networks. *Neuroimage* 2009;44:715-723
 40. Song J, Birn RM, Boly M, Meier TB, Nair VA, Meyerand ME, et al. Age-related reorganizational changes in modularity and functional connectivity of human brain networks. *Brain Connect* 2014;4:662-676
 41. Alexander-Bloch AF, Gogtay N, Meunier D, Birn R, Clasen L, Lalonde F, et al. Disrupted modularity and local connectivity of brain functional networks in childhood-onset schizophrenia. *Front Syst Neurosci* 2010;4:147
 42. Brier MR, Thomas JB, Fagan AM, Hassenstab J, Holtzman DM, Benzinger TL, et al. Functional connectivity and graph theory in preclinical Alzheimer's disease. *Neurobiol Aging* 2014;35:757-768
 43. Baum GL, Ciric R, Roalf DR, Betzel RF, Moore TM, Shinohara RT, et al. Modular segregation of structural brain networks supports the development of executive function in youth. *Curr Biol* 2017;27:1561-1572.e8
 44. Sporns O. The non-random brain: efficiency, economy, and complex dynamics. *Front Comput Neurosci* 2011;5:5
 45. Nakayama N, Okumura A, Shinoda J, Yasokawa YT, Miwa K, Yoshimura SI, et al. Evidence for white matter disruption in traumatic brain injury without macroscopic lesions. *J Neurol Neurosurg Psychiatry* 2006;77:850-855
 46. Eierud C, Craddock RC, Fletcher S, Aulakh M, King-Casas B, Kuehl D, et al. Neuroimaging after mild traumatic brain injury: review and meta-analysis. *Neuroimage Clin* 2014;4:283-294
 47. Akiki TJ, Averill CL, Wrocklage KM, Scott JC, Averill LA, Schweinsburg B, et al. Default mode network abnormalities in posttraumatic stress disorder: a novel network-restricted topology approach. *Neuroimage* 2018;176:489-498
 48. Zhou Y. Small world properties changes in mild traumatic brain injury. *J Magn Reson Imaging* 2017;46:518-527
 49. Kaushal M, España LY, Nencka AS, Wang Y, Nelson LD, McCrea MA, et al. Resting-state functional connectivity after concussion is associated with clinical recovery. *Hum Brain Mapp* 2019;40:1211-1220
 50. Vakhtin AA, Calhoun VD, Jung RE, Prestopnik JL, Taylor PA, Ford CC. Changes in intrinsic functional brain networks following blast-induced mild traumatic brain injury. *Brain Inj* 2013;27:1304-1310